Characterization of the Fast Neutron Generators for Calibration of Fusion Neutron Diagnostics

T. Kormilitsyn[1,*], A. Pankratenko[1], Yu. Kashchuk[1], S. Obudovsky[1], R. Rodionov[1], D. Fridrikhsen[1], A. Krasilnikov[1], S. Syromukov[2], D. Yurkov[2]
[1]Project Center ITER (ITER RF DA), Moscow, Russia
[2]Dukhov Automatics Research Institute (FSUE VNIIA), Moscow, Russia
(*) t.kormilitsyn@iterrf.ru

Abstract*—Modern magnetic confinement fusion devices increasingly rely on extensive neutron diagnostic configurations to measure a plethora of key plasma parameters. Measurement accuracy for these diagnostics depends heavily on in situ calibration. In order to enable said calibration, we set out to propose a reliable and powerful fast neutron source, to define a characterization plan for this source in terms of yield, flux and energy distributions, propose an optimized set of tools suitable for online monitoring of neutron source performance and its metrological characteristics. In the framework of this research activity with the ultimate aim of ITER tokamak neutron diagnostics calibration we rely on industrial-grade fast neutron generator NG-24 (D-D neutron yield ~10^9 n/s, D-T neutron yield ~10^{11} n/s) with sealed tube and stuffed, titanium target developed by FSUE VNIIA. The well-known analytical expressions for thick target NGs and our measurements using neutron spectrometers utilizing threshold reactions – diamond detector and $LaCl_3$ scintillator for D-T and D-D neutron generators respectively – were found to be significantly coherent. These data are supported through our multi-step forward modelling including ion stopping in target, fusion reaction kinematics modelling and calculating detector response based on modelled neutron spectra. We discuss methods of uncertainty mitigation of neutron spectrometer measurements. Application of both neutron activation analysis and gas-filled neutron flux monitors during source characterization and operation allows for lowing statistical uncertainty of neutron flux measurements to 1% level over 1 minute of time resolution. Over the course of several measurement campaigns the optimal set of measurement tools have been determined including detector dimensions, required acquisition time, calibration methods.

***Keywords* — neutron generator, neutron spectrometer, fusion product, plasma diagnostics, neutron calibration.**

I. Introduction

The task of fusion neutron diagnostic calibration consists of a continuous set of challenges including factory calibration of the diagnostic equipment, on-site testing and commissioning activities, *in situ* calibration with fast neutron source and cross-calibration during discharges. The objectives of current work revolve around characterization of a chosen source with proven reliability and suitable for the *in situ* neutron calibration activity.

Several aspects limit the choice of the fast neutron source for this task – available space, project schedule, cost, safety considerations and, of course, source neutron spectra. Majority of calibration campaigns of the operating magnetic confinement fusion devices relied on isotope sources, including JET [1], Globus-M2 [2] and TFTR [3]. Only recently the calibration campaign at JET [4] had made use of compact sealed tube neutron generators (NGs) [5] to significant success. The key advantages of the modern sealed tube NGs are:

- neutron spectrum consistent with fusion neutrons for both deuterium and deuterium-tritium plasma scenarios;
- togglable operation without unnecessary irradiation going on during source transportation, storage, handling and between expositions;
- point-like source (Ø2 cm) with yield of D-D and D-T neutrons comfortably reaching the yield of 10^9 and 10^{11} n/s respectively;
- modest weight (<200 kg) and dimensions (<Ø50×115cm) that correspond well to the Type-A package required for transportation and handling of ^{252}Cf source with comparable yield (10^9 n/s).

The main disadvantages of this source type include – neutron yield and energy anisotropy and (for high-yield models) the need for active target cooling. Said disadvantages are an additional source of measurement error for the diagnostics undergoing the calibration, and the goal of characterization of sealed tube NG is elimination of this error.

The NG yield determination for both D-D and D-T cases requires relevant measurement techniques that allow for both time-resolved monitoring and absolute measurement of the number of neutrons produced by the source. The robust tools suitable for monitoring of fast neutron flux include threshold fission chambers [6,7] and gas counters based on boron [8] and helium-3 [9]. Neutron activation analysis (NAA) technique is deemed the fusion industry standard for absolute measurements of neutron yield during discharge [10,11] and can be confidently applied for the task of characterization of a fast neutron source.

Given the nature of fusion reaction kinematics [12] the change in average neutron energy with respect to beam direction will present a significant source of uncertainty. Hence, to maximize the confidence and precision of the calibration we propose to apply for both tasks – source characterization and

© The Authors, published by EDP Sciences. This is an open access article distributed under the terms of the Creative Commons Attribution License 4.0 (https://creativecommons.org/licenses/by/4.0/).

subsequent monitoring – a set of neutron spectrometers with the goal of determination of neutron energy distribution. For the D-D NG the detector of choice is $LaCl_3$ scintillator [13,14] with fast neutron detection via the $^{35}Cl(n,p)^{35}S_{g.s.}$ reaction, for the D-T NG – diamond detector with its respective $^{12}C(n,\alpha)^{9}Be$ [15,16] reaction. Both of these instruments allow for pulse-height analysis and feature a classical gaussian-shape response to fast neutrons. This approach allowed us to study the neutron energy distribution at various angle to the ion beam and thus verify the assumptions embedded in the forward modeling of the experiment.

II. Measurement Setup

The measurement setup required for characterization of the fusion neutron source is formed by the source itself – the neutron generator, the neutron spectrometers typically located within 50 cm from the target due to their low sensitivity, neutron monitors – gas-filled ionization chambers – located at a higher distance to avoid pulse pileup. The neutron activation system is constituted of gamma-ray spectrometer and a pneumatic system delivering activation samples to and from the irradiation zone. Coverage of several neutron emission angles with spectrometers is achieved using an automated positioning system operated, together with NG and measurement system I&C from a secure control room.

A. Neutron generator

Considering the dimensions of ITER machine with major radius exceeding 6 m and minor – exceeding 2 m [17], we provision the use of NG-24 neutron generator manufactured by FSUE VNIIA [18], the main technical specifications of this model are listed in Table I.

TABLE I
NG-24 KEY TECHNICAL SPECIFICATIONS

Quantity	Value	
Dimensions, mm	Ø430×1150	
Weight, kg	175	
Sealed tube lifetime, hrs	300	
Ion source, type	Penning	
Ion current, mA	Up to 2	
Accelerating voltage, kV	Up to 250	
Modification	D-T	D-D
Ion beam composition	D^+, T^+, D_2^+, T_2^+, DT^+	D^+, D_2^+
Neutron yield, n/s	$\sim10^{11}$	$\sim10^{9}$
Average neutron energy at 90°, MeV	~14.1	~2.45

The sketch of the NG irradiation unit is illustrated in Several details that constitute the know-how of the manufacturer were omitted. The key element of the NG is the sealed tube and the detailed design around the radiative spot – NG target – has been thoroughly modelled for further research to include the copper cooling circuit, stuffed, titanium target, and sealed tube housing. The supporting structure for the scintillator-based neutron spectrometer to be located in the frontal sphere of the NG has also been designed.

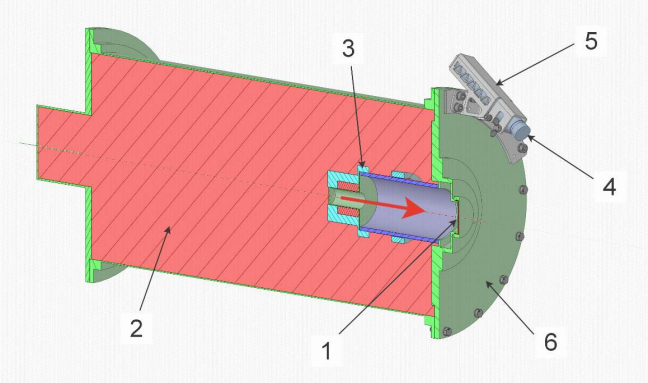

Fig. 1. Vertical cross-section of the simplified neutron generator CAD model. Red arrow shows ion beam direction. 1 – Ti target, 2 – transformer oil (CH_2), 3 – magnets, 4 – sensitive element of neutron spectrometer, 5 – detector support structure, 6 – neutron generator flange.

The duration of expositions necessary for the successful calibration of the key ITER neutron diagnostics lie in the order of hours [19], hence, a 1-minute time resolution for measurements of NG yield and energy we presume sufficient. The tests of the NG-24 model for yield stability measured using laboratory helium-3 neutron counter have yielded good results of only ±2,5% yield change over 1 shift (7 hr 30 min) of continuous operation. Test results further underline the lack of necessity to further minimize the time resolution.

B. Neutron monitors

The task of determination of NG yield starts with determination of neutron flux at detector location. This section comprises a brief overview of achievable results with regard to determination of neutron flux value at several suitable locations around NG irradiation unit.

For this, in D-D NG case operating with the yield of $\sim10^9$ n/s, the boron gas-filled counter is deemed most suitable. Given the Q = 2792 keV the $^{10}B(n,\alpha)^{7}Li$ reaction with the cross-section at E_n = 2.5 MeV reaching 1 barn, this monitor is highly sensitive to both thermal and D-D neutrons. With a fairly unsophisticated I&C system this sensor constitutes a robust solution achieving $>10^4$ counts per minute at locations near the front on the NG. The sensor mass being as low as 12 g allows designating its location near the back side of the front NG flange on the outer wall of the NG housing. Nevertheless, its sensitivity to thermal neutrons requires mitigation using shielding materials to prevent counts from backscattered fast neutrons. The low abundance of helium-3 [20] and the need increase bias voltage for detector operation (1200 V versus 500 V) rule out the use of said counters for the task of D-D NG characterization and monitoring during operation.

The D-T NG with the yield being 2 orders of magnitude higher ($\sim10^{11}$ n/s) over the D-D modification, allows for use of the threshold fission chambers (FC) with radiators covered by uranium-238 [21]. The FC with 0.5 g of fissile material operating at 300 V of bias voltage is a perfect candidate for NG monitoring purposes due to reaction threshold (~1 MeV) and due to the cross-section increasing with energy up to 2 barn for E_n = 14 MeV. FC location directly behind the back flange of the NG allows reaching count-rates above 10^4 per minute, lowering

the statistical uncertainty of flux reconstruction down to 1%.

C. *Neutron activation analysis*

The more precise way to provide absolute measurements of the neutron yield integrated over time is the use of neutron activation technique also applicable to magnetic confinement fusion devices [10,11,22]. For this, we have utilized several activation samples listed in the Table II with the key characteristics derived based on ENDF-B/V.III [23].

TABLE II
KEY CHARACTERISTICS OF THE MATERIAL SAMPLES USED FOR NAA

Sample	Indium	Cadmium	Aluminum	Teflon
Source	D-D		D-T	
Process	^{115}In(n,n')^{115m}In	^{111}Cd(n,n')^{111m}Cd	^{27}Al(n,α)^{24}Na	^{19}F(n,2n)^{18}F
Q, MeV	-1.5	-0.4	-3.132	-10.431
σ,barn	0.327	0.239	0.118	0.057
$T_{1/2}$, hrs	4.486	0.81	14.887	1.829
Eγ, keV / Eff. %	336 / 45.9	245 / 94	1369 / 99.99 2754 / 99.985	511 / 193.46

The D-D neutron energy range ~ 2.5 MeV is covered with only a few threshold reactions occurring in common NAA samples. The two select isotopes feature a gamma-ray energy of the same order of magnitude, but vastly different thresholds, with ^{115}In cross-section more closely matching the required range [24]. In laboratory conditions under the sealed tube D-D neutron generator operating at accelerating voltage of 150 kV, 150 μA of ion current amounting to 10^7 n/s yield the irradiation time required exceeded 10 hours for a 0.2 g sample located at 1.5 cm away from NG target. Increasing the yield to NG-24 operation parameters, increasing the distance to ~50 cm and increasing the weight of the sample tenfold would amount to the same irradiation time needed to achieve the same 3% of statistical uncertainty in neutron fluence determination. This leaves little room for application of NAA technique for detailed multi-angle characterization of the source, but the technique still remains crucial for absolute scaling of measurements by neutron flux monitors and spectrometers provisioned for characterization and monitoring of the D-D NG.

Precise D-T NG yield determination requires less irradiation time and allows the use of samples more fit for purpose of NAA. The pure aluminum sample allows measurements using two gamma-ray energies, further lowering statistical uncertainty. The Teflon sample while having lower cross-section has a more favorable threshold reaching slightly above 10 MeV. The use of these samples with characteristic weight of 1 g under irradiation using NG-24 D-T model operating at 200 kV of accelerating voltage, 2 mA of ion current and producing ~5×10^{10} n/s allowed determination of the local D-T neutron flux with the accuracy within 2% after 1 hour of irradiation.

Activation of each sample has been studied with the laboratory Ø2×2-inch $LaBr_3$(Ce) scintillator calibrated using a set of standard ^{60}Co, ^{137}Cs and ^{22}Na isotope sources.

The NAA technique highlighted in this section provides an independent and robust measurement of the absolute neutron flux value necessary to minimize the final uncertainty of NG parameters after characterization.

III. NEUTRON SPECTROMETER RESULTS AND DISCUSSION

A. *Chlorine-based neutron spectrometer*

Recent developments in the field of fast neutron spectrometry have led to a series of scintillating materials being utilized due to availability of ^{35}Cl(n,p)^{35}S$_{g.s.}$ (Q=615 keV, σ=0.15 barn for E_n = 2.5 MeV) reaction for measurement of fast neutrons. For the purposes of neutron generator characterization and consequent monitoring we propose the $LaCl_3$(Ce) scintillator, having in mind the previous multi-step modelling and analysis of experiment with a low-power NG yielding promising results [25]. With the light yield being higher and with response being faster than that of CLYC crystals, this detector looks most promising for operation in the harsh environment – within 50 cm and in direct view of the D-D NG target. The pulse-shape discrimination capability of $LaCl_3$(Ce) is lower than that of CLYC (Figure-of-Merit = 1.0 versus >2.0) and requires digitization of the signal with sampling rate of at least 500 MSps at 14-bit resolution. The detector energy resolution in our previous work was estimated at 8% [26].

We coupled the Ø2×0.5-inch crystal to the Hamamatsu R6231-100 PMT and conducted a series of expositions at a fixed distance of 43.5 cm from the target center of D-D modification of the NG-24 operating at 220 kV of accelerating voltage and 1 mA of ion current which corresponds to 5×10^8 n/s yield. The only parameter varying in between the expositions was the angle between the detector line of sight and the NG axis. Following the digital pulse-shape discrimination procedure (PSD) [27], we conducted the pulse-height analysis of the detector pulses, associated with slowing down of protons born in the (n,p)-reaction for each of the expositions. The results are illustrated on Fig. 2.

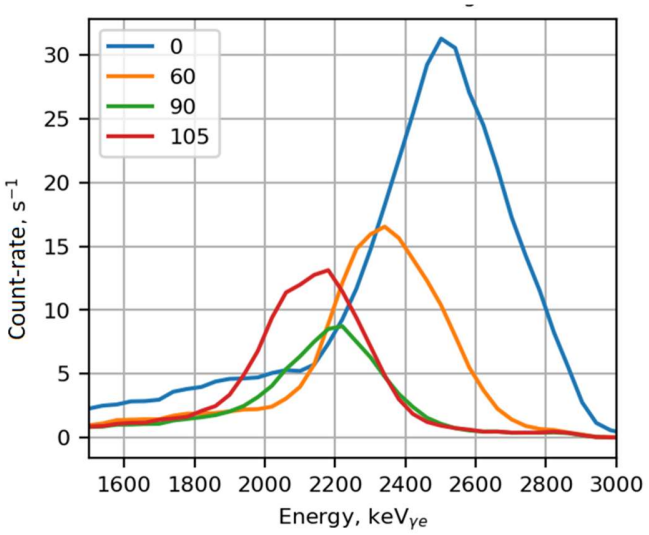

Fig. 2. Pulse-height analysis of proton-associated events in the $LaCl_3$(Ce) response after PSD plotted for several angles between detector line-of-sight and NG axis, calibrated in the gamma-ray equivalent energy.

The figure-of-merit of current crystal sample was found to be lower and averaged at 0.45 across the expositions, this is primarily due to increased ^{227}Ac contamination [28] of the

crystal compared to previously used samples. At the same time, background radiation arising from this contamination in the form of α-decay events was recorded in between each irradiation for the duration of ~5 minutes. No visible deviation has been found in the shape of the pulse-height distribution or the position of the α-decay event peaks. This fortunate circumstance allowed us to self-calibrate the detector using known locations of the peaks, and continue to monitor the energy calibration stability between each exposition. Using the p/β-ratio derived from the previous measurements (~0.75) and (n,p)-reaction kinematics allowed us to infer average neutron energies for each of the irradiation angles. The results of the measurement are summarized in the Fig. 3 and Table III. The agreement between measurement and the data for thick targets by J. Csikai [29] is within 2%.

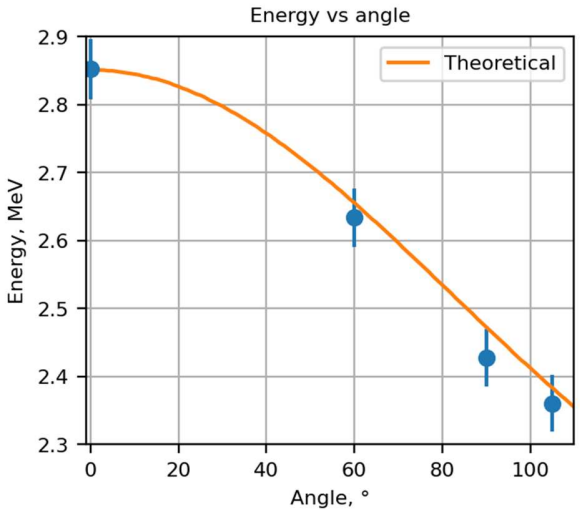

Fig. 3. Neutron energy measured using $LaCl_3(Ce)$ versus the angle plotted against analytical approximation of thick target NG data.

TABLE III
NG NEUTRON ENERGY MEASUREMENT VERSUS THICK-TARGET DATA

Angle, °	Average E_n, Analytical approximation [29], keV	Average E_n, $LaCl_3$ measurement, keV
0	2851	2852±45
60	2656	2634±43
90	2473	2428±42
105	2384	2361±42

The absolute measurements of neutron flux is undermined by discrepancies in the cross-section data for the $^{35}Cl(n,p)$ reactions in the literature [23,30,31]. Experiment data yield incoherent results in terms of absolute yield reconstruction and requires further investigation using a metrological fast neutron source.

Detector performance in terms of relative measurements and average neutron energy determination is on substantial level, allowing it to be used as a primary tool for both characterizing the NG and monitoring its performance during operation. Provisioned placement of $LaCl_3(Ce)$-based detector in the frontal sphere of the NG within 50 cm of its target allows reaching count rates above 10^4 events per minute in the (n,p)-associated peak without significant pulse pileup and PSD degradation, which is effectively aligns with results of the experimental campaign.

B. Diamond neutron spectrometer

The semiconductor detector based on a CVD-diamond mono-crystal is a widely adopted [32-35] method for measurement of D-T neutron energy and flux. Having a high critical fluence of ~10^{14} n/cm^2 and impeccable energy resolution ~1% this detector highly benefits form predominantly (except for impurities) carbon composition and a threshold reaction that produces a classical gaussian-like response – $^{12}C(n,\alpha)^9Be$, Q=-5.7 MeV.

Utilizing the 4×4×0.5 mm^3 crystal coupled to a Canberra 2004 preamplifier, Ortec 673 Amplifier and Ortec 926 analyzer we have conducted a set of measurements at 10 cm from the target of the the NG-24 (D-T modification) operating at 200 kV of accelerating voltage and 0.5 mA of ion current, corresponding to the yield of ~2×10^{10} n/s. Detector energy calibration was performed using isotope source of α-particles ^{226}Ra and its analytically estimated sensitivity is ~6×10^{-5} cm^2.

This set of measurements allowed us to study the change in the pulse-height distribution with the angle between detector LOS and NG axis. The PHA of detector for various irradiation angles is illustrated on Fig. 4 with each exposition time being equal to 180 s.

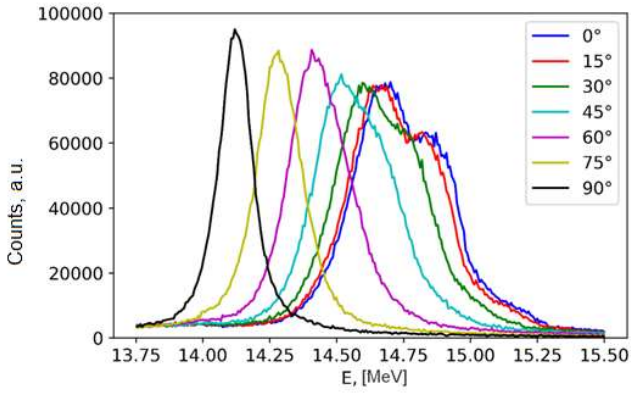

Fig. 4. Diamond detector PHA under D-T NG irradiation plotted for various angles between detector LOS and NG axis, exposition time = 180 s.

Verification of measurement results was done for two critical location – 0 and 90 degrees. For this, we utilized the multi-step modelling approach briefly described in [36]. The neutron generator beam ion composition was presumed 90% molecular ions (45% DT^+, 22.5% D_2^+, 22.5% T_2^+ and 10% single (5% D^+ and 5% T^+). The ranges for stopping of said ions were calculated using SRIM software for the titanium bulk material, each ion had its velocity vector recorded, with that, beam-target reaction kinematics was calculated and the resulting neutron energy and angle distribution was modelled. Beam component-wise energy distribution of the neutrons born in the direction along the NG axis is illustrated on Fig. 5.

The resulting energy distribution convoluted with (n,α)-reaction cross-section was plotted against the results obtained

in experiment and shows significant coherence in shape and absolute number of events as illustrated on Fig. 6.

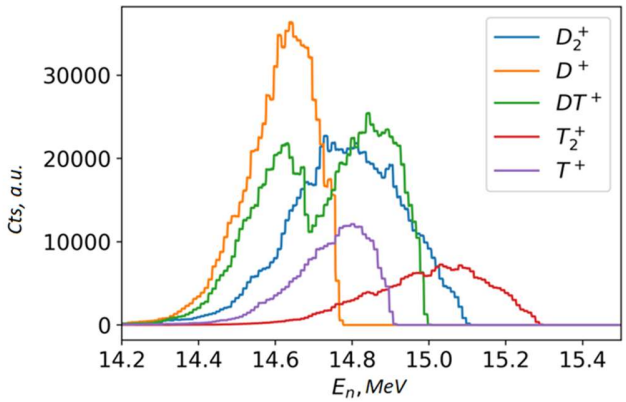

Fig. 5. Diamond detector PHA under D-T NG irradiation plotted for various components of the ion beam for the detector LOS along NG axis, exposition time = 180 s.

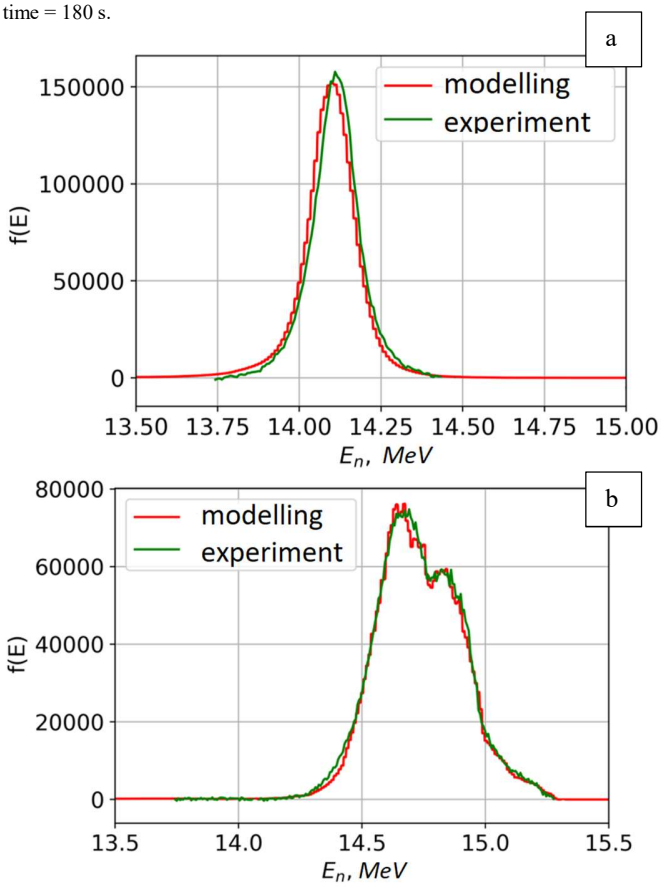

Fig. 6. Comparison between measured detector response and multi-step modelling results for the same experiment. (a) – 0-degree direction, (b) – 90-degree direction.

Diamond detector performance for the purposes of characterizing the D-T NG demonstrates stellar results. With that, its location within 30 cm from target of D-T NG operating at 10^{11} n/s leads to a count rate of the order 5×10^3 per second and its increase would likely constitute a pulse pileup due to significant number of pulses occurring at lower amplitudes simultaneously. The statistical uncertainty in determination of local neutron flux achievable over 1 minute of spectra integration time falls well below 1% in this case nevertheless.

IV. Conclusions and Outlook

In present work we outline the set of key tools necessary for conversion of the industrial-grade sealed tube neutron generator into metrological source fit for calibration and testing of the fusion neutron diagnostics.

Based on extensive experience of operation of sealed tube NGs our recommendation is to use multi-vector approach with simultaneous measurements done by means of neutron activation samples, conventional neutron monitors and unique neutron spectrometers, thus allowing to cover both the absolute neutron fluence measurements, consistent neutron flux monitoring and detailed energy versus angle characterization of the source.

Tests in laboratory conditions allow us to pinpoint the optimal sensor locations for each type of the source provisioned to be used in the ITER calibration campaigns – the sealed tube NG-24 neutron generator. The increase of the number of sensors in each case is a subject to a detailed reliability study.

For D-D source (yield 10^9 n/s) the boron counters are to be located directly behind the front flange of the NG, on the outer surface of the NG body, with careful consideration of the shielding conditions. The neutron spectrometer suitable for both characterization and subsequent monitoring is the lanthanum chloride scintillator, shown able to consistently (<2%) determine the average energy and therefore monitor the stability of NG accelerating voltage. The location in the frontal sphere within 40-50 cm range will allow to drive the statistical uncertainty of neutron flux determination based on this set of two tools well below 1% over each minute of the ongoing exposition.

For D-T source (yield 10^{11} n/s) the uranium-238 fission chambers are a robust tool that may be located behind the back flange of the NG. This location will also require careful design of shielding to prevent backscatter counts. The diamond neutron spectrometer seems a perfect candidate for monitoring of both neutron flux and neutron spectrum from a location in the frontal sphere of the NG. The low dimensions of diamond detector (2-3 cm^3) constitute very little obstruction to the diagnostics undergoing calibration. The cumulative statistical uncertainty of neutron flux determination of this set of tools also reach values well below 1% over 1 minute of irradiation.

The multi-step modelling approach developed and tested over the span of these experiment campaigns provided us with important insight into NG performance and verified a set of measurements of both diamond and chlorine-based neutron spectrometers. The sum total of modelling the ion stopping in the target and the beam-target reaction kinematics allows for analytical definition of the NG source that is both usable in future modelling and is consistent with the measurements.

Acknowledgment

This work has been funded under the Implementing Agreement No. 1 (ITER ref. IO/21/CT/4300002349) between Institution ‘‘Project Center ITER’’ and the ITER International

Fusion Energy Organization "Research and Detailed Design Development of the components needed for Neutron Generators suitable for ITER in-situ neutron calibration''.

ITER is the Nuclear Facility INB no. 174. The views and opinions expressed herein do not necessarily reflect those of the ITER Organization.

DATA AVAILABILITY STATEMENT

The data that support the findings of this study are available from the corresponding author upon reasonable request.

REFERENCES

[1] O. Jarvis, G. Sadler, P. Van Belle, T. Elevant (1990) In-vessel calibration of the JET neutron monitors using a 252Cf neutron source: Difficulties experienced. Rev Sci Instrum 61:3172–3174. DOI: 10.1063/1.1141677
[2] O. Skrekel, N. Bakharev, V. Varfolomeev, et al (2022) Calibration of neutron counters at the Globus-M2 tokamak. Tech Phys 92:12. DOI: 10.21883/TP.2022.01.52526.151-21
[3] H. Hendel, R. Palladino, C. Barnes, et al (1990) In situ calibration of TFTR neutron detectors. Rev Sci Instrum 61:1900–1914. DOI: 10.1063/1.1141115
[4] P. Batistoni, S. Popovichev, Z. Ghani, et al (2018) 14 MeV calibration of JET neutron detectors - Phase 2: In-vessel calibration. Nucl Fusion 58:106016. DOI: 10.1088/1741-4326/aad4c1
[5] Yu. Kaschuck, D. Portnov, A. Krasilnikov, et al (1999) Compact neutron generator for diagnostic applications. Rev Sci Instrum 70:1104–1106. DOI: 10.1063/1.1149473
[6] Yu. Kashchuk, V. Shevchenko, V. Frunze, A. Krasil'nikov. (2005) Monitoring the fast-neutron flux density and fluence in a RBMK core using a threshold fission chamber in a screen-absorber. At Energy 98:249–255. DOI: 10.1007/S10512-005-0202-X/
[7] L. Bertalot, R. Barnsley, F. Direz, et al (2012) Fusion neutron diagnostics on ITER tokamak. J Instrum 7:C04012. DOI: 10.1088/1748-0221/7/04/C04012
[8] P. Dighe, D. Prasad, K. Prasad, et al (2003) Boron-lined proportional counters with improved neutron sensitivity. Nucl Instruments Methods Phys Res Sect A Accel Spectrometers, Detect Assoc Equip 496:154–161. DOI: 10.1016/S0168-9002(02)01635-2
[9] R. Batchelor (1952) Neutron energy measurements with a helium 3 filled proportional counter, Proc. Phys. Soc. Sect. A 65:674–675
[10] R. Prokopowicz, B. Bienkowska, K. Drozdowicz, et al (2011) Measurements of neutrons at JET by means of the activation methods. Nucl Instruments Methods Phys Res Sect A Accel Spectrometers, Detect Assoc Equip 637:119–127. DOI: 10.1016/j.nima.2011.01.128
[11] C. Barnes, M. Loughlin, T. Nishitani (1997) Neutron activation for ITER. Rev Sci Instrum 68:577–580. DOI: 10.1063/1.1147657
[12] H. Brysk (1973) Fusion neutron energies and spectra. Plasma Phys 15:611–617. DOI: 10.1088/0032-1028/15/7/001
[13] T. Kormilitsyn, S. Obudovsky, Yu. Kashchuk, et al (2021) Application of the LaCl3(Ce) Scintillator to Fast Neutron Measurements. Phys Part Nucl Lett 18:75–81. DOI: 10.1134/S154747712101009X
[14] P. Vuong, H. Kim, N. Luan, S. Kim (2021) Neutron spectroscopy using pure LaCl3 crystal and the dependence of pulse shape discrimination on Ce-doped concentrations. Nucl Eng Technol 53:3784–3789. DOI: 10.1016/J.NET.2021.05.020
[15] A. Krasilnikov (1998) Natural Diamond Neutron Spectrometer. In: Diagnostics for Experimental Thermonuclear Fusion Reactors 2. Springer US, Boston, MA, pp 439–448
[16] A. Krasilnikov, V. Amosov, P. Van Belle, et al (2002) Study of d-t neutron energy spectra at JET using natural diamond detectors. Nucl Instruments Methods Phys Res Sect A Accel Spectrometers, Detect Assoc Equip 476:500–505. DOI: 10.1016/S0168-9002(01)01497-8
[17] K. Ioki, C. Choi, E. Daly, et al (2012) ITER Vacuum Vessel design and construction. Fusion Eng Des 87:828–835. DOI: 10.1016/j.fusengdes.2012.02.023
[18] S. Syromukov, V. Stepnov, R. Dobrov, et al (2015) NG-24 Neutron Generator for Nuclear Medicine and Thermonuclear Research. At Energy 119:68–71. DOI: 10.1007/s10512-015-0031-5
[19] T. Nishitani, M. Ishikawa, ML.-S. Cheon, et al (2023) Neutronic simulations of in-vessel neutron calibrations for ITER neutron diagnostics by using simplified ITER model. Fusion Eng Des 191:113548. DOI: 10.1016/j.fusengdes.2023.113548
[20] R. Kouzes, A. Lintereur, E. Siciliano (2015) Progress in alternative neutron detection to address the helium-3 shortage. Nucl Instruments Methods Phys Res Sect A Accel Spectrometers, Detect Assoc Equip 784:172–175. DOI: 10.1016/j.nima.2014.10.046
[21] S. Obudovskii, A. Batyunin, V. Sevast'yanov, et al (2016) Metrological Assurance of Thermonuclear Neutron Flux Density Measurements. Meas Tech 59:288–292. DOI: 10.1007/s11018-016-0960-y
[22] M. Hoek, T. Nishitani, Y. Ikeda, A. Morioka (1995) Neutron yield measurements by use of foil activation at JT-60U. Rev Sci Instrum 66:885–887. DOI: 10.1063/1.1146527
[23] D. Brown, M. Chadwick, R. Capote, et al (2018) ENDF/B-VIII.0: The 8th Major Release of the Nuclear Reaction Data Library with CIELO-project Cross Sections, New Standards and Thermal Scattering Data. Nucl Data Sheets 148:1–142. DOI: 10.1016/j.nds.2018.02.001
[24] C. Duniiu, Y. Baosheng, L. Hanlin, Z. Wenrong, 115In(n,n')115mIn cross section evaluation, INDC(CPR) 024/L, (1991), IAEA
[25] T. Kormilitsyn, S. Obudovsky, R. Rodionov, et al (2021) Novel LaCl3(Ce)-based spectrometer for deuterium plasma neutron diagnostics. Rev Sci Instrum 92:043528. DOI: 10.1063/5.0042394
[26] V. Pankratenko, T. Kormilitsyn, Yu. Kashuck, et al (2023) Analysis of the LaCl3(Ce) scintillator response function to fast neutrons. Nucl Instruments Methods Phys Res Sect A Accel Spectrometers, Detect Assoc Equip 1052:168282. DOI: 10.1016/j.nima.2023.168282
[27] A. Pankratenko, T. Kormilitsyn, S. Obudovsky, et al (2022) Digital Pulse Shape Discrimination Method for D–D Neutron Spectrometry Using the LaCl3(Ce) Scintillator. Phys Part Nucl Lett 19:66–76. DOI: 10.1134/S1547477122010095
[28] W. Wolszczak, P. Dorenbos (2017) Shape of intrinsic alpha pulse height spectra in lanthanide halide scintillators. Nucl Instruments Methods Phys Res Sect A Accel Spectrometers, Detect Assoc Equip 857:66–74. DOI: 10.1016/j.nima.2017.02.041
[29] J. Csikai (1987) CRC handbook of fast neutron generators; 240 p; CRC Press Inc; Boca Raton, FL (USA)
[30] S. Kuvin, H. Lee, T. Kawano, et al (2020) Nonstatistical fluctuations in the Cl 35 (n,p) S 35 reaction cross section at fast-neutron energies from 0.6 to 6 MeV. Phys Rev C 102:024623. DOI: 10.1103/PhysRevC.102.024623
[31] J. Batchelder et al (2019). Possible evidence of nonstatistical properties in the Cl 35 (n, p) S 35 cross section, Physical Review C, 99(4). DOI: 10.1103/PhysRevC.99.044612
[32] L. Bertalot, J. Adams, M. Angelone, et al (2005) ITER relevant developments in neutron diagnostics during the JET Trace Tritium campaign. In: Fusion Engineering and Design. North-Holland, pp 835–839, DOI: 10.1016/j.fusengdes.2005.06.213
[33] G. Ericsson G. (2019) Advanced Neutron Spectroscopy in Fusion Research. J Fusion Energy 38:330–355. DOI: 10.1007/s10894-019-00213-9
[34] C. Cazzaniga, M. Nocente, M. Rebai, et al (2014) A diamond-based neutron spectrometer for diagnostics of deuterium-tritium fusion plasmas. Rev Sci Instrum 85:11E101. DOI: 10.1063/1.4885356
[35] B. Esposito, D. Marocco, G. Gandolfo, et al (2022) Progress of Design and Development for the ITER Radial Neutron Camera. J Fusion Energy 41:22. DOI: 10.1007/s10894-022-00333-9
[36] T. Kormilitsyn, S. Obudovsky, Yu. Kashchuk, et al (2021) Application of the LaCl3(Ce) Scintillator to Fast Neutron Measurements. Phys Part Nucl Lett 18:75–81. DOI: 10.1134/S154747712101009X